Electrical Power and Energy Systems 104 (2019) 279–290

Contents lists available at ScienceDirect

Electrical Power and Energy Systems

journal homepage: www.elsevier.com/locate/ijepes

A reserve capacity model of AA-CAES for power system optimal joint energy and reserve scheduling

Yaowang Li[a], Shihong Miao[a,*], Shixu Zhang[a], Binxin Yin[a], Xing Luo[a,b], Mark Dooner[b], Jihong Wang[a,b]

[a] State Key Laboratory of Advanced Electromagnetic Engineering and Technology, Hubei Electric Power Security and High Efficiency Key Laboratory, School of Electrical and Electronic Engineering, Huazhong University of Science and Technology (HUST), Wuhan, China
[b] School of Engineering, University of Warwick, Coventry, UK

ARTICLE INFO

Keywords:
Advanced adiabatic compressed air energy storage (AA-CAES)
Reserve capacity
Power system scheduling
Optimization

ABSTRACT

Advanced Adiabatic Compressed Air Energy Storage (AA-CAES) has received much attention in the recent years due to its merits of no fossil fuel consumption, low costs, fast start-up and wide-ranging part load ability. It is considered to have a variety of power gird applications including providing reserve services. Although a number of studies are reported in the optimal scheduling strategy of using compressed air energy storage, very few studies have been reported in AA-CAES reserve capacity modelling. This paper presents a reserve capacity model for an AA-CAES facility considering its working mode conversion process, the dynamic characteristics, the air pressure limitations, the thermal storage capacity limitations and the power output limitations of AA-CAES. The developed reserve capacity model is then used in the power system optimal joint energy and reserve scheduling. In the scheduling, the limits on the reserve capacities of Thermal Power Units (TUs) and Interruptible Loads (ILs), which are caused by AA-CAES, are taken into account. The developed scheduling model are used to analyse the impacts of AA-CAES on the system energy and reserve schedules, the system operation costs and the wind curtailment. Numerical simulation results indicate that the participation of AA-CAES in power system operation does not only reduce the system energy and reserve costs, but also mitigate the wind curtailment. However, it is found that AA-CAES is unsuitable for undertaking the system reserve demand alone and using AA-CAES to provide reserve services may increase the system total reserve demand.

1. Introduction

Wind power generation is growing rapidly around the world, due to its environmentally friendly and fossil fuel saving benefits [1–2]. However, the intermittency and uncertainty of wind power bring technical and economical challenges to power systems [3]. Recently, Electrical Energy Storage (EES) such as Compressed Air Energy Storage (CAES) [2], Pumped Hydro Storage (PHS) [4], batteries [5], pumped thermal electricity storage [6–8] and liquid air energy storage [9] have attracted much attention in addressing the challenges of large-scale wind power grid integration. Among various technologies of ESS, PHS and CAES are two proven technologies suitable for large-scale storage applications [10,11]. However, further implantation of PHS is limited by its requirement for suitable geographical conditions and potential ecological damage. Compared to PHS, CAES has fewer construction constraints, lower costs and causes less damage to ecology [12]. Therefore, CAES, as a promising large-scale EES technology, is considered as an alternative to PHS. [13].

The operation of a Conventional Compressed Air Energy Storage (C-CAES) is similar to a conventional gas turbine with the compression and generation stages occurring independently [14]. There are two successfully commercial C-CAES plants in the world. The first is the 290 MW Huntorf plant in Germany. The other is the 110 MW McIntosh plant in the US [10]. However, the main drawbacks of C-CAES plants are that the cycle efficiency is relatively low and the fossil fuel consumption is required in the discharging stage. For improving these disadvantages, Advanced Adiabatic Compressed Air Energy Storage (AA-CAES) system is developed. AA-CAES can extract heat from the air compression stage and store it in an adiabatic reservoir. Then, the heat can be reused during the expansion stage [15]. Fig. 1 illustrates a schematic layout of a typical AA-CAES system, which is composed of a multi-stage air compression unit (low pressure and high pressure compressors), a multi-stage air expansion unit (low pressure and high pressure turbines), electric motor/generator, Heat Exchangers (HEXs),

* Corresponding author.
E-mail address: shmiao@hust.edu.cn (S. Miao).

https://doi.org/10.1016/j.ijepes.2018.07.012
Received 11 April 2018; Received in revised form 13 June 2018; Accepted 5 July 2018
Available online 14 July 2018
0142-0615/

Nomenclature

A. Indices

t	index of time
k	index of compressor
j	index of turbine
i	index of TU
x	index of IL
z	index of TL
n	index of outage TU
b	index of bus
l	index of transmission line

B. Sets

T	set of time periods
n_c	set of compressors
n_g	set of turbines
N_G	set of TUs
N_{TL}	set of TLs
N_{IL}	set of ILs
$T_{TL,x}$	set of time at which the operation of TL x can be scheduled
B	set of buses
L	set of transmission lines

C. Parameters

γ	specific heat ratio of air
R_g	universal gas constant
$c_{p,air}$	specific heat capacity of air
ε	the HEX effectiveness
η_c/η_g	isentropic efficiency of compression and generation stages
$T_{c,k,in}/T_{g,j,in}$	inlet temperature of compressor k and turbine j at rated condition
$\beta_{c,k}/\beta_{g,j}$	rated pressure ratio of compressor k and turbine j
$T_{st,in}$	average air temperature at the entrance of the air reservoir
V_{st}	volume of the air reservoir
T_{wall}	wall temperature of the air reservoir
α_h/β_h	effective heat transfer coefficients
T_{hot}/T_{cold}	temperature of the hot and cold TES working medium
$p_{st,0}$	the initial air pressure in the air reservoir
$Q_{HS,0}$	initial stored heat in the heat reservoir
Δt	unit scheduling period
$\Delta t_5/\Delta t_{15}$	5 min and 15 min
$P_{CAESC,\min}/P_{CAESC,\max}$	lower and upper limits of the compressing power
$P_{CAESG,\min}/P_{CAESG,\max}$	lower and upper limits of the generating power
$p_{st,\min}/p_{st,\max}$	upper and lower limits of the air pressure in the air reservoir
$\overline{Q}_{HS}$	upper limit of the thermal storage capacity
$\Delta t_{C,on}/\Delta t_{G,on}$	the time that the AA-CAES facility switches from the idling mode to the minimum compression and minimum generation
$\Delta t_{C,off}/\Delta t_{G,off}$	the time that the AA-CAES facility switches from the minimum compression and minimum generation to the idling mode
$r^{up}_{CAESG}/r^{up}_{CAESC}$	ramp up rate in the generation mode and compression mode
$r^{down}_{CAESG}/r^{down}_{CAESC}$	ramp down rate in the generation mode and compression mode
μ_{re}	proportion of gas reduction by using the heat recuperator
A_{gas}	heat value of gas
η_{gas}	combustion efficiency of gas
b_{Gi}/c_{Gi}	energy cost coefficients of TU i
b_{CAES}	energy cost coefficient of the AA-CAES facility
α_{Gi}/β_{Gi}	cost coefficients of providing upward and downward regulation reserves by TU i
$\gamma_{Gi}/\gamma_{CAES}/\gamma_{IL,z}$	cost coefficients of providing contingency reserve by TU i, the AA-CAES facility and IL z
$b_{TL,x}$	load-shifting cost of TL x
λ_w	penalty of wind curtailment
$P_{W,t}$	wind power forecast output at time t
$P_{L,t}$	forecast load at time t
$\varepsilon_{L,t}$	load forecast error at time t
$\varepsilon_{W,t}$	wind power forecast error at time t
$e_{L,t}$	standard deviation of load forecast error at time t
$e_{W,t}$	standard deviation of wind power forecast error at time t
μ	risk level
$D^{+}_{TLx,\max}/D^{-}_{TLx,\max}$	maximum load increment and reduction of TL x
$Q_{TLx,\max}$	maximum total schedulable load of TL x
$IL_{z,\max}$	maximum contingency reserve of IL z
$Q_{ILx,\max}$	maximum total schedulable load of IL z
$P_{Gi,\min}/P_{Gi,\max}$	upper and lower limit of TU i
r^{up}_G/r^{down}_G	maximum ramp up and down rate of TU i
M^{ON}_{Gi}/M^{OFF}_{Gi}	minimum ON/OFF time of TU i
F_{lb}	line flow distribution factor for the transmission line l linking bus b, due to net injection at bus b [1]
$L_{l,\max}$	maximum transmission capacity for the transmission line l

D. Variables

$P_{CAESC,t}/P_{CAESG,t}$	compressing and generating power of CAES at time t
$v_{c,t}/v_{g,t}$	unit state indicator in generation and compression modes at time t (1 is ON and 0 is OFF).
$\dot{p}_{st,t}$	change rate of air pressure in the air
air	reservoir at time t
$p_{st,t}$	air pressure in the air reservoir at time t
$P_{Qc,t}/P_{Qg,t}$	heat transfer power of the HEX during the compression stage and the expansion stage at time t
$T_{st,t}$	air temperature inside the air reservoir
$Q_{HS,t}$	stored heat in the heat reservoir
$\dot{m}_{c,t}/\dot{m}_{g,t}$	mass flow rate in compression and generation stages at time t
$P^{\underline{p}}_{CAESG,t}/P^{\underline{Q}}_{CAESG,t}$	maximum generating power limited by the lower limits of air pressure and thermal storage capacity
$P^{\overline{p}}_{CAESC,t}/P^{\overline{Q}}_{CAESC,t}$	maximum compressing power limited by the upper limits of air pressure and thermal storage capacity
$R^{Rup}_{CAES,t}/R^{Rdown}_{CAES,t}$	upward and downward regulation reserves of AA-CAES at time t
$R^{C}_{CAES,t}$	contingency reserve of AA-CAES at time t
$P'_{Qg,t}$	heat transfer power in combustion chamber at time t
$C_{C-CAESg,t}$	gas consumption cost of C-CAES at time t
$P_{Gi,t}$	output power of TU i at time t
$S_{Gi,t}$	start-up cost of TU i
$u_{Gi,t}$	unit state indicator of TU at time t (1 is ON and 0 is OFF).
$R^{Rup}_{Gi,t}/R^{Rdown}_{Gi,t}$	upward and downward regulation reserves provided by TU i at time t
$R^{C}_{Gi,t}/R^{C}_{ILz,t}$	contingency reserve provided by TU i and IL z at time t
$d^{+}_{TLx,t}/d^{-}_{TLx,t}$	load increment and load reduction of TL x at time t
W_t	wind curtailment at time t
$R^{+,\min}_{G,t}$	minimum upward regulation reserve provided by TUs or the minimum contingency reserve provided by TUs and ILs
$R^{-,\min}_{G,t}$	minimum downward regulation reserve provided by Tus
P^{b}_{t}	net injection at bus b at time t

E. Abbreviations

EES	electrical energy storage
CAES	compressed air energy storage
C-CAES	conventional compressed air energy storage
AA-CAES	Advanced adiabatic compressed air energy storage
PHS	pumped hydro storage
TU	thermal power unit
TL	time-shifting load
IL	interrupt load
HEX	heat exchanger
TES	thermal energy storage
MINLP	mixed integer non-linear programming
MILP	mixed integer linear programming

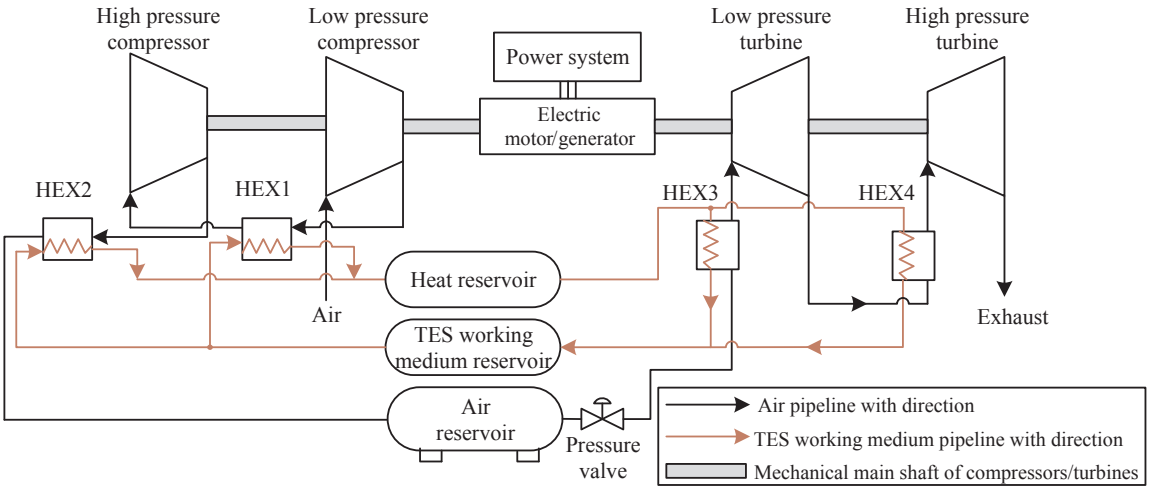

Fig. 1. Schematic diagram of an AA-CAES facility (HEX-heat exchanger, TES-thermal energy storage) [15].

a heat reservoir, a Thermal Energy Storage (TES) working medium reservoir, and an air reservoir. During the compression stage, electricity is used for air compression. The high pressure air is stored in the air reservoir while the compression heat is stored in the heat reservoir. During the expansion process, the stored heat is reused to heat the pressurized air in HEXs, and then, the heated compressed air is used to drive a multi-stage turbine for electricity generation [15].

At present, a number of AA-CAES demonstration plants are under development or in the early stage of experiment worldwide. The world's first large scale AA-CAES demonstration plant – ADELE – is in the development stage, at Saxony-Anhalt in Germany. The plant was designed to have a storage capability of 360 MWh and an electricity output of 90 MW, aiming for 70% cycle efficiency [15]. In China, a 500 kW demonstration AA-CAES system, named TICC-500, was built and passed various load tests [16]. The Institute of Engineering Thermophysics, Chinese Academy of Sciences built one 1.5 MW AA-CAES demonstration facility located near Beijing, China and another 10 MW/40 MW.h AA-CAES demonstration plant is in Guizhou, China [17]. In addition, a 50 MW AA-CAES project began in Jiangsu, China, and a 100 MW AA-CAES system will be built after the study from the 50 MW system [18].

The significant research work has been conducted in the optimal operation strategy of C-CAES. The bidding and offering strategy of C-CAES is studied in [19–21]. With the consideration of the electricity market price as an uncertain parameter, an offering and biding strategy for the merchant C-CAES using robust optimization approach was proposed by Nojavan et al. [19]. Shafiee et al. proposed an information gap decision theory based risk-constrained bidding/offering strategy for a C-CAES plant considering price forecasting errors [20]. They also presented an algorithm to construct hourly bidding and offering curves to purchase and sell electricity for a price-maker C-CAES facility participating in a day-ahead electricity market [21].

The self-scheduling strategy of C-CAES in the electricity market is studied in [22–26]. Li et al. proposed an optimal self-scheduling strategy for a wind generation and C-CAES combined system to increase the combined system revenue [22]. Attarha et al. proposed an adaptive robust self-scheduling model for a wind producer paired with a C-CAES system considering the uncertainties of wind power productions and price forecast errors [23]. A joint operation framework considering PHS, CAES and wind farms was presented by Wang et al. [24], and an optimal self-scheduling model for the joint operation system for mitigating wind curtailment was also proposed in this paper. A optimal self-scheduling strategy for the generation company with a C-CAES facility as well as thermal power units, renewable resources and demand side resources were studied in [25,26].

The optimal energy scheduling strategies for power systems with C-CAES has been studied in [27,28]. Daneshi et al. presented an approach for security constrained unit commitment with the integration of a C-CAES plant [27]. The impacts of C-CAES system on locational pricing, economics, peak-load shaving, environmental perspective and wind curtailment were analysed as well [27]. Ghaljehei et al. proposed a stochastic security constrained unit commitment model integrating C-CAES in a power system with wind power [28]. A practical criterion of the static voltage stability was considered as an operational constraint in the developed model [28].

The above literatures indicate that C-CAES has the capability of mitigating wind curtailment, providing load shifting service and reducing the system operation cost, but the performance of C-CAES in providing reserve services was not analysed. Compared to C-CAES, AA-CAES has a higher cycle efficiency with no fossil fuel consumption. It also has distinguished merits of high ramp up/down rates, wide-ranging part load and fast start-up/shut down ability [3,10]. Thus, AA-CAES can be considered as a good option to provide reserve services with low operating cost [29]. The operating reserves are vital to the power system as they are used to ensure the power system operation reliability [30]. Also, a more effective and accurate reserve scheduling model can lead to higher economic benefits for the system operator. Therefore, for maximizing both technical and economic benefits of AA-CAES, the study of the energy and reserve scheduling model for AA-CAES operation is quite important.

However, there are very limited studies that focus on the reserve scheduling of AA-CAES systems and the optimal joint energy and reserve scheduling method for the power system with AA-CAES. Li et al. proposed a dispatch model of zero-carbon-emission micro energy internet with a micro AA-CAES [31]. The article only presented an energy management model of a micro AA-CAES. The reserve characteristics are not considered. Shafiee et al. developed an energy and reserve self-scheduling model for a merchant C-CAES facility considering its thermodynamic characteristics [32]. However, the proposed reserve capacity model cannot be applied to an AA-CAES facility because the thermal storage capacity limits of the AA-CAES was not considered. Also, the working mode conversion process and dynamic characteristics of C-CAES are neglected in the proposed model. Drury et al. developed a simplified energy and reserve self-scheduling model for C-CAES and AA-CAES to quantify their potential value in several US markets [29]. The proposed reserve capacity model can be used for the overall economic analysis, but it is less accurate enough for power system day-ahead scheduling as it only takes maximum compressing and generating power limits into account.

From the above, the practical limitations and operation characteristics of AA-CAES were not fully considered in the proposed reserve capacity models, and there is no research about energy and reserve scheduling of the power system with AA-CAES. So, in this paper, a the reserve capacity model for AA-CAES considering its working modes conversion process, the dynamic characteristics, the air pressure limits, thermal storage capacity limits and output limits is developed. Then, an optimal joint energy and reserves scheduling model for the power system with an AA-CAES facility is proposed.

The contributions of this paper are highlighted as follows: 1) The first regulation and contingency reserve capacity model for AA-CAES is developed, which considering the working mode conversion process, dynamic characteristics, air pressure limits, thermal storage capacity limits and output limits of AA-CAES. 2) A novel joint energy and reserve optimal scheduling model for the power system containing the AA-CAES, Thermal Power Units (TUs), the wind power plant, Time-shifting Loads (TLs) and Interrupt Loads (ILs) is developed. The limitations on the reserve capacities of TUs and ILs caused by the AA-CAES are taken into account in the scheduling model. 3) Based on the developed scheduling model, the impacts of AA-CAES on system operation costs, wind curtailment, energy schedules and reserve schedules are analysed, and the impacts of AA-CAES and C-CAES on system operation costs and reserve schedules are compared.

The rest of the paper is organized as follows. In Section 2, the model formulation of AA-CAES systems for energy and reserve scheduling is presented. In Section 3, the comparison of AA-CAES and C-CAES in energy and reserve scheduling model is carried out. In Section 4, the optimal joint energy and reserve scheduling model for power system with the AA-CAES is presented. In Section 5, case studies and simulation discussions are provided. Finally, Section 6 concludes the paper.

2. Model formulation of AA-CAES systems for energy and reserve scheduling

This section is separated into two parts. In Subsection 2.1, the formulation of AA-CAES energy scheduling model is present. In Subsection 2.2, the main factors that limit the reserve capacity of AA-CAES are analysed, and the reserve capacity model of AA-CAES is presented.

2.1. Modelling of AA-CAES energy scheduling constraints

In this subsection, a thermodynamic model of an AA-CAES system is used to calculate its operation conditions. The operation conditions include mass flow rate, air pressure in the air reservoir, heat transfer power and stored heat in the heat reservoir. Subsequently, the practical operation constraints of AA-CAES are formulated.

1) Modelling of AA-CAES operation conditions

A thermodynamic model of AA-CAES is used in this paper to calculate the operation conditions of AA-CAES system. The compressing power and generating power are calculated by (1) and (2), respectively [15]. Considering the heat transfer between the air reservoir and the atmosphere, the change rate of air pressure in the air reservoir can be calculated by (3) [10]. The air pressure in the air reservoir is described by (4). The HEX effectiveness is used into determine the heat transfer of a HEX, and the heat transfer power of HEXs during the compression stage and the expansion stage can be described by (5) and (6), respectively [15,31]. The stored heat in the heat reservoir is calculated by (7).

$$P_{CAESC,t}\eta_c = \dot{m}_{c,t}\frac{\gamma}{\gamma-1}R_g\left[\sum_{k=1}^{n_c} T_{c,k,in}\left(\beta_{c,k}^{\frac{\gamma-1}{\gamma}}-1\right)\right], \quad \forall\, t \in T \tag{1}$$

$$P_{CAESG,t} = \eta_g \dot{m}_{g,t}\frac{\gamma}{\gamma-1}R_g\sum_{j=1}^{n_g} T_{g,j,in}\left(1-\beta_{g,j}^{-\frac{\gamma-1}{\gamma}}\right), \quad \forall\, t \in T \tag{2}$$

$$\dot{p}_{st,t} = \frac{R_g T_{st,in}\gamma}{V_{st}}\dot{m}_{c,t} - \frac{R_g T_{st,t}\gamma}{V_{st}}\dot{m}_{g,t} - (\alpha_h + \beta_h|\dot{m}_{c,t}-\dot{m}_{g,t}|^{0.8})(T_{st,t} - T_{wall}), \quad \forall\, t \in T \tag{3}$$

$$p_{st,t} = p_{st,0} + \sum_{\tau=1}^{t}\dot{p}_{st,\tau}\Delta t, \quad \forall\, t \in T \tag{4}$$

$$P_{Qc,t} = \dot{m}_{c,t}c_{p,air}\varepsilon\left(\sum_{k=1}^{n_c} T_{c,k,in}\beta_{c,k}^{\frac{\gamma-1}{\gamma}} - n_c T_{cold}\right), \quad \forall\, t \in T \tag{5}$$

$$P_{Qg,t} = \dot{m}_{g,t}c_{p,air}\varepsilon\left(n_g T_{hot} - T_{st,t} - \sum_{j=1}^{n_g-1} T_{g,j,in}\beta_{g,j}^{-\frac{\gamma-1}{\gamma}}\right), \quad \forall\, t \in T \tag{6}$$

$$Q_{HS,t} = Q_{HS,0} + \sum_{\tau=1}^{t} P_{Qc,\tau}\Delta t - \sum_{\tau=1}^{t} P_{Qg,\tau}\Delta t, \quad \forall\, t \in T \tag{7}$$

2) Practical operation constraints of AA-CAES

The limits on the compressing power and generating power are presented in (8) and (9), respectively. The limit on the air pressure in the air reservoir is presented in (10). The limit on the thermal storage capacity of the heat reservoir is described by (11). Since the compression and generation modes do not occur simultaneously [2], (12) is used to model the limit.

$$P_{CAESC,\min}v_{c,t} \leqslant P_{CAESC,t} \leqslant P_{CAESC,\max}v_{c,t}, \quad \forall\, t \in T \tag{8}$$

$$P_{CAESG,\min}v_{g,t} \leqslant P_{CAESG,t} \leqslant P_{CAESG,\max}v_{g,t}, \quad \forall\, t \in T \tag{9}$$

$$p_{st,\min} \leqslant p_{st,t} \leqslant p_{st,\max}, \quad \forall\, t \in T \tag{10}$$

$$0 \leqslant Q_{HS,t} \leqslant \overline{Q}_{HS}, \quad \forall\, t \in T \tag{11}$$

$$v_{c,t} + v_{g,t} \leqslant 1, \quad \forall\, t \in T \tag{12}$$

It should be noted that, since the CAES plant can switch from full generation to full compression (or full compression to full generation) within a scheduling period (15 min) [3]. The ramp rate constraint of the CAES plant can be ignored in the day-ahead scheduling.

2.2. Reserve capacity model of AA-CAES

In this subsection, the main factors which limit the reserve capacity of AA-CAES are analysed. Based on the analysis, the regulation and contingency reserve capacity models of AA-CAES are formulated.

1) Analysis on the main factors which limit the reserve capacity of AA-CAES

Reserve is the idle capacity which provides for unexpected load (or wind power output) variations and generator outages. The first objective is attained with the *regulation reserve* while the second is attained with the *contingency reserve* [30]. The upward and downward regulation reserve should restrain the power variation in 5 min, while the contingency reserve should compensate the loss of generating power in 15 min [33].

The main factors which limit the AA-CAES reserve capacity are listed and analysed:

a. *The dynamic characteristics:* Normally, a CAES facility can swing from full generation to full compression in less than 5 min, and back to full generation in less than 15 min [3], which means a CAES facility can change its working modes during the process of providing reserve services to achieve better reserve-providing ability. Therefore, the dynamic characteristics, such as ramp-up/down rates, start-up/shut-down time can limit the reserve capacity of AA-CAES.
b. *Upper and lower limits of compressing and generating power:* The maximum upward power regulation of AA-CAES is limited by the maximum generating power and minimum compressing power, while the maximum downward power regulation of AA-CAES is limited by the minimum generating power and maximum compressing power. Therefore, the reserve capacity of AA-CAES can be limited by the limits of the compressing and generating power.
c. *The limits on the air pressure in the air reservoir:* When the air pressure is close to its upper limit, the compressing power is limited by the maximum air pressure. When the air pressure is close to its lower limit, the generating power is limited by the minimum air pressure.
d. *The limits on the thermal storage capacity in the heat reservoir:* Similarly, when the stored heat is close to the limits, the compressing and generating power are limited by the upper and lower limits of the thermal storage capacity, respectively.
e. *The operation conditions:* AA-CAES has different power regulation capabilities under different operation conditions. For example: An AA-CAES operating in generation mode can downregulate much more output power than an AA-CAES which is operating in compression mode (the compressing power can be taken as negative generating power). Therefore, the operation conditions of AA-CAES have a great effect on the reserve capacity of AA-CAES.

2) Regulation reserve capacity model of AA-CAES

When an AA-CAES facility is operating in compression mode and is going to provide upward regulation reserve, it has 3 options: 1) maintaining compression mode and downregulating the compressing power; 2) switching to idling mode; 3) switching to generation mode and generating power. According to the analysis in the previous subsection, the limits on the upward regulation reserve under the above 3 options can be modelled by (13)(15). Whereas, when an AA-CAES facility is going to provide downward regulation reserve, it has to maintain the compression mode and upregulate the compressing power. The limit on the downward regulation reserve capacity is modelled by (16).

$$0 \leqslant R_{CAES,t}^{Rup} \leqslant P_{CAESC,t} - P_{CAESC,\min}, \quad \forall\, t \in T \tag{13}$$

$$R_{CAES,t}^{Rup} = P_{CAESC,t}, \quad \forall\, t \in T \tag{14}$$

$$P_{CAESC,t} + P_{CAESG,\min} \leqslant R_{CAES,t}^{Rup} \leqslant P_{CAESC,t} + \min\left[\left(\Delta t_5 - \frac{P_{CAESC,t}}{r_{CAESC}^{down}} - \Delta t_{G,on} - \Delta t_{C,off}\right) r_{CAESG}^{up} + P_{CAESG,\min},\ P_{CAESG,\max},\ P_{CAESG,t}^{P},\ P_{CAESG,t}^{Q}\right], \quad \forall\, t \in T \tag{15}$$

$$0 \leqslant R_{CAES,t}^{Rdown} \leqslant \min(P_{CAESC,\max},\ P_{CAESC,t}^{\overline{P}},\ P_{CAESC,t}^{\overline{Q}}) - P_{CAESC,t}, \quad \forall\, t \in T \tag{16}$$

When an AA-CAES facility is operating in idling mode, it has to switch to generation and compression modes to provide upward and downward regulation reserves, respectively. The constraints are modelled by (17) and (18), respectively.

$$P_{CAESG,\min} \leqslant R_{CAES,t}^{Rup} \leqslant \min[(\Delta t_5 - \Delta t_{G,on}) r_{CAESG}^{up} + P_{CAESG,\min},\ P_{CAESG,\max},\ P_{CAESG,t}^{P},\ P_{CAESG,t}^{Q}], \quad \forall\, t \in T \tag{17}$$

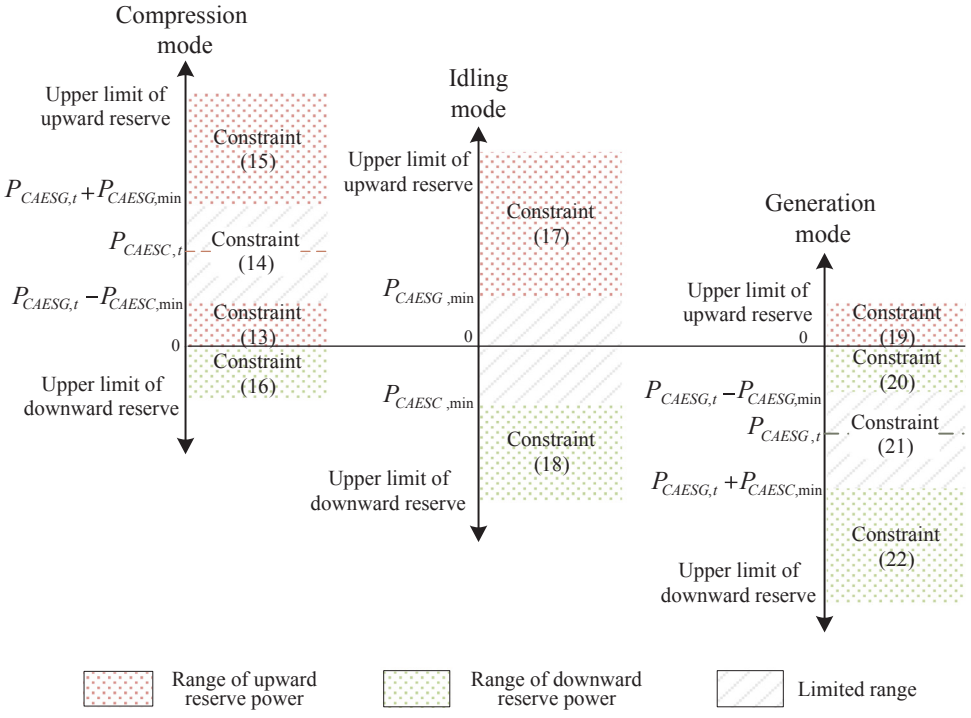

Fig. 2. Regulation range of the upward and downward regulation reserve capacity.

$$P_{CAESC,\min} \leqslant R^{Rdown}_{CAES,t} \leqslant \min[(\Delta t_5 - \Delta t_{C,on}) r^{up}_{CAESC} + P_{CAESC,\min}, P_{CAESC,\max}, P^{\overline{P}}_{CAESC,t}, P^{\overline{Q}}_{CAESC,t}], \quad \forall t \in T \tag{18}$$

Similarly, when an AA-CAES is operating in generation mode, the limits on upward and downward regulation reserves can be modelled by (19) and (20)(22), respectively.

$$0 \leqslant R^{Rup}_{CAES,t} \leqslant \min(P_{CAESG,\max}, P^{P}_{CAESG,t}, P^{Q}_{CAESG,t}) - P_{CAESG,t}, \quad \forall t \in T \tag{19}$$

$$0 \leqslant R^{Rdown}_{CAES,t} \leqslant P_{CAESG,t} - P_{CAESG,\min}, \quad \forall t \in T \tag{20}$$

$$R^{down}_{CAES,t} = P_{CAESG,t}, \quad \forall t \in T \tag{21}$$

$$P_{CAESG,t} + P_{CAESC,\min} \leqslant R^{Rdown}_{CAES,t} \leqslant P_{CAESG,t} + \min\left[\left(\Delta t_5 - \frac{P_{CAESG,t}}{r^{down}_{CAESG}} - \Delta t_{G,off} - \Delta t_{C,on}\right) r^{up}_{CAESC} + P_{CAESC,\min}, P_{CAESC,\max}, P^{\overline{P}}_{CAESC,t}, P^{\overline{Q}}_{CAESC,t}\right], \quad \forall t \in T \tag{22}$$

In summary, the regulation range of the upward and downward regulation reserve is illustrated in Fig. 2. The upper limit of the upward reserve is limited by the dynamic characteristics, the maximum generating power, the lower limit of air pressure and the lower limit of the thermal storage capacity. Meanwhile, the upper limit of the downward reserve is limited by the dynamic characteristics, the maximum compressing power, the upper limit of air pressure and the upper limit of the thermal storage capacity.

It should be note that the regulation range of the reserve capacity provided by AA-CAES is not continuous (see Fig. 2) due to the lower limits of compressing and generating power. The impacts of this working characteristic on the reserve capacities of TUs and ILs are analysed in Section 4.2.

3) Contingency reserve capacity model of AA-CAES

Normally, an AA-CAES facility can swing from full compression to full generation within 15 min [3]. Therefore, the dynamic characteristics can be ignored in the contingency reserve capacity model of AA-CAES. Similar to the model formulation of the upward regulation reserve capacity, the limits on the contingency reserve capacity can be modelled by (23)(27).

$$0 \leqslant R^{C}_{CAES,t} \leqslant P_{CAESC,t} - P_{CAESC,\min}, \quad \forall t \in T \tag{23}$$

$$R^{C}_{CAES,t} = P_{CAESC,t}, \quad \forall t \in T \tag{24}$$

$$P_{CAESC,t} + P_{CAESG,\min} \leqslant R^{C}_{CAES,t} \leqslant P_{CAESC,t} + \min(P_{CAESG,\max}, P^{P}_{CAESG,t}, P^{Q}_{CAESG,t}), \quad \forall t \in T \tag{25}$$

$$P_{CAESG,\min} \leqslant R^{C}_{CAES,t} \leqslant \min(P_{CAESG,\max}, P^{P}_{CAESG,t}, P^{Q}_{CAESG,t}), \quad \forall t \in T \tag{26}$$

$$0 \leqslant R^{C}_{CAES,t} \leqslant \min(P_{CAESG,\max}, P^{P}_{CAESG,t}, P^{Q}_{CAESG,t}) - P_{CAESG,t}, \quad \forall t \in T \tag{27}$$

Note that, the day-ahead scheduling is the first stage of the multi-time scale scheduling. There are other scheduling resources such as fast start-up generators which can be used for power regulation in the intra-day scheduling or real-time dispatch [34]. Also, the extreme situation does not usually occur. Therefore, to achieve higher benefits in the day-ahead scheduling, the simultaneous occurrence of a single TU outage and the power shortage is not considered, meanwhile the simultaneous occurrence of multi generator outages is also not considered in the paper.

3. Comparison of AA-CAES and C-CAES in energy and reserve scheduling model

In this section, the differences between AA-CAES and C-CAES in energy and reserve scheduling modelling are analysed. Subsequently, the model formulation of C-CAES in energy and reserve scheduling is presented.

The main difference between an AA-CAES and a C-CAES is that C-CAES has a combustion chamber and uses natural gas to heat the high pressure air, while AA-CAES uses TES for heat storage and reuse [15]. Therefore, the constraints related to TES, which are expressed by (5)(7) and (11), are not included in the energy scheduling model of C-CAES. But all other constraints of AA-CAES including (1)(4), (8)(10) and (12) are included in the energy scheduling model of C-CAES. Apart from this, the operation constraints related with the combustion process are included. The heat-producing power from the gas combustion is calculated by (28). The gas consumption cost of C-CAES is calculated by (29) [22].

$$P'_{Qg,t} = \dot{m}_{g,t} c_{p,air} (1 - \mu_{re}) \left(\sum_{j=1}^{n_g} T_{g,j,in} - \sum_{j=1}^{n_g - 1} T_{g,j,in} \beta_{g,j}^{-\frac{\gamma-1}{\gamma}} - T_{st,t} \right), \quad \forall t \in T \tag{28}$$

$$C_{C-CAESg,t} = \frac{P'_{Qg,t}}{A_{gas} \eta_{gas}} c_{gas} \Delta t, \quad \forall t \in T \tag{29}$$

Since C-CAES does not have TES, the thermal storage capacity is no longer one of the main factors which limits reserve capacity. The regulation reserve constraints of C-CAES comprise (13)(22) and the following modifications: The $P^{Q}_{CAESG,t}$ in (15), (17) and (19) are deleted and the $P^{\overline{Q}}_{CAESC,t}$ in (16), (18) and (22) are deleted. Similarly, the contingency reserve constraints of C-CAES comprise (23)(27) and the following modifications: The $P^{Q}_{CAESG,t}$ in (25)(27) are deleted.

Although the formulations of C-CAES and AA-CAES reserve capacity models are similar, the parameters in the two models can be different. For example, compared to AA-CAES, C-CAES normally takes more time to start-up because of the gas combustion process [3,35]. Also, the cost of providing reserve by C-CAES is higher than AA-CAES [29].

4. Optimal joint energy and reserve scheduling model for the power system with an AA-CAES

In this section, an optimal joint energy and reserve scheduling model is proposed for the power system with an AA-CAES. The demand response programs are used in the power system to make TLs and ILs schedulable. The TL's operation can be scheduled any time within a given time frame for providing load-shifting service, while the ILs can be used to provide contingency reserve service [36,37]. The following scheduling resources are included in the power system: TUs, an AA-CAES facility, a wind farm, TLs and ILs. In order to mitigate wind curtailment, the wind power is assumed to have the highest scheduling priority.

4.1. Objective function

The objective is to minimize the power system operation cost over the next 24 h. The objective function is formulated as (30). The first and second terms account for the energy costs of TUs and the AA-CAES facility. The third and fourth terms represent the regulation reserve cost and the contingency reserve cost of TUs. The fifth and sixth terms represent the regulation reserve cost and the contingency reserve cost of the AA-CAES facility. The seventh and eighth terms account for the

scheduling costs of TLs and ILs. The final term is the punishment cost for wind curtailment.

$$\min \sum_{t=1}^{T}\sum_{i=1}^{N_G}(b_{Gi}P_{Gi,t}\Delta t + c_{Gi} + S_{Gi,t}) + \sum_{t=1}^{T} b_{CAES}P_{CAESG,t}\Delta t + \sum_{t=1}^{T}\sum_{i=1}^{N_G}(\alpha_{Gi}R_{Gi,t}^{Rup} + \beta_{Gi}R_{Gi,t}^{Rdown}) + \sum_{t=1}^{T}\sum_{i=1}^{N_G}\gamma_{Gi}R_{Gi,t}^{C} + \sum_{t=1}^{T}(\alpha_{CAES}R_{CAES,t}^{Rup} + \beta_{CAES}R_{CAES,t}^{Rdown}) + \sum_{t=1}^{T}\gamma_{CAES}R_{CAES,t}^{C} + \sum_{t=1}^{T}\sum_{x=1}^{N_{TL}}(d_{TLx,t}^{+} + d_{TLx,t}^{-})b_{TL,x}\Delta t + \sum_{t=1}^{T}\sum_{z=1}^{N_{IL}}R_{ILz,t}^{C}\gamma_{IL,z} + \sum_{t=1}^{T}\lambda_w W_t\Delta t \tag{30}$$

4.2. Modelling the limits on reserve capacity caused by AA-CAES

In this subsection, the limits on reserve capacity of TUs and ILs caused by AA-CAES are analysed and modelled.

It can be observed from Fig. 2 that, if the system reserve demand is completely undertaken by AA-CAES, the power variation cannot be fully restrained when the system reserve demand is just in the "blanks" of the regulation range (see unfeasible range I-VI in Fig. 2). Therefore, TUs and ILs should provide enough reserves to fill in the "blanks". According the above analysis, the limits on the reserve capacity of TUs and ILs caused by AA-CAES can be modelled by (31)(33).

$$\sum_{i=1}^{N_G} R_{Gi,t}^{Rup} \geqslant R_{G,t}^{+,\min}, \quad \forall\, t \in T \tag{31}$$

$$\sum_{i=1}^{N_G} R_{Gi,t}^{Rdown} \geqslant R_{G,t}^{-,\min}, \quad \forall\, t \in T \tag{32}$$

$$\sum_{i=1,i\neq n}^{N_G} R_{Gi,t}^{C} + \sum_{z=1}^{N_{IL}} R_{ILz,t}^{C} \geqslant R_{G,t}^{+,\min}, \quad \forall\, t \in T, \forall\, n \in N_G \tag{33}$$

According to Fig. 2, when AA-CAES is operating in compression mode and switches to generation and idling modes to provide reserve services, $R_{G,t}^{+,\min}$ can be calculated by (34) and (35), respectively. When AA-CAES is operating in idling mode and switches to generation and compression modes to provide reserve services, $R_{G,t}^{+,\min}$ and $R_{G,t}^{-,\min}$ can be calculated by (36) and (37), respectively. When AA-CAES is operating in generation mode and switches to compression and idling modes to provide reserve services, $R_{G,t}^{-,\min}$ can be calculated by (38) and (39), respectively. In other conditions, $R_{G,t}^{+,\min}$ and $R_{G,t}^{-,\min}$ are equal to 0.

$$R_{G,t}^{+,\min} = \max(P_{CAESG,\min}, P_{CAESC,\min}), \quad \forall\, t \in T \tag{34}$$

$$R_{G,t}^{+,\min} = P_{CAESC,\min}, \quad \forall\, t \in T \tag{35}$$

$$R_{G,t}^{+,\min} = P_{CAESG,\min}, \quad \forall\, t \in T \tag{36}$$

$$R_{G,t}^{-,\min} = P_{CAESC,\min}, \quad \forall\, t \in T \tag{37}$$

$$R_{G,t}^{-,\min} = \max(P_{CAESG,\min}, P_{CAESC,\min}), \quad \forall\, t \in T \tag{38}$$

$$R_{G,t}^{-,\min} = P_{CAESG,\min}, \quad \forall\, t \in T \tag{39}$$

4.3. Other constraints

In this subsection, the power balance constraint, system reserve constraints, TLs constraints, ILs constraints, TUs constraints and the transmission line capacity constraint are presented. Note that the constraints of AA-CAES are presented in Section 2, modelled by (1)(22).

1) *Power balance constraint*

$$\sum_{i=1}^{N_G} P_{Gi,t} + P_{W,t} + P_{CAESG,t} + \sum_{x=1}^{N_{TL}} d_{TLx,t}^{-} - W_t = P_{L,t} + P_{CAESC,t} + \sum_{x=1}^{N_{TL}} d_{TLx,t}^{+}, \quad \forall\, t \in T \tag{40}$$

2) *System reserve constraints*

The system operator has to purchase enough regulation reserve and contingency reserve to ensure the reliable operation of the power system. The total required regulation reserve is mainly affected by the wind power and load forecast errors. Assuming that the load forecast error ($\varepsilon_{L,t}$) and wind power forecast error ($\varepsilon_{W,t}$) are represented by normal distributions where the means are 0 and the standard deviations are $e_{L,t}$ and $e_{W,t}$ respectively [38]. The constraints of total required regulation reserve are modelled by (41), (42). These two constraints are used to make sure that the system operator purchases enough regulation reserve. The total required contingency reserve is mainly affected by the output power of the operating TUs. The constraint of total required contingency reserve is modelled by Eq. (43). The constraint is used to make sure the power system has the ability to overcome a set of single TU outage.

$$\Pr\{\sum_{i=1}^{N_G} R_{Gi,t}^{Rup} + R_{CAES,t}^{Rup} \geqslant \varepsilon_{L,t} - \varepsilon_{W,t}\} \geqslant 1-\mu, \quad \forall\, t \in T \tag{41}$$

$$\Pr\{\sum_{i=1}^{N_G} R_{Gi,t}^{Rdown} + R_{CAES,t}^{Rdown} \geqslant \varepsilon_{W,t} - \varepsilon_{L,t}\} \geqslant 1-\mu, \quad \forall\, t \in T \tag{42}$$

$$\sum_{i=1,i\neq n}^{N_G} R_{Gi,t}^{C} + R_{CAES,t}^{C} + \sum_{z=1}^{N_{IL}} R_{ILz,t}^{C} \geqslant P_{Gn,t}, \quad \forall\, t \in T, \forall\, n \in N_G \tag{43}$$

3) *TL constraints*

The maximum load increment and reduction constraints are described by (44), (45). Eq. (46) ensures the electricity consumption of TLs remain unchanged after the scheduling. The maximum total schedulable load constraint of TLs is described by (47).

$$0 \leqslant d_{TLx,t}^{+} \leqslant D_{TLx,\max}^{+}, \quad \forall\, t \in T_{TL,x}, \forall\, x \in N_{TL} \tag{44}$$

$$0 \leqslant d_{TLx,t}^{-} \leqslant D_{TLx,\max}^{-}, \quad \forall\, t \in T_{TL,x}, \forall\, x \in N_{TL} \tag{45}$$

$$\sum_{t=1}^{T} d_{TLx,t}^{+} - \sum_{t=1}^{T} d_{TLx,t}^{-} = 0, \quad \forall\, x \in N_{TL} \tag{46}$$

$$\sum_{t=1}^{T} d_{TLx,t}^{-}\Delta t \leqslant Q_{TLx,\max}, \quad \forall\, x \in N_{TL} \tag{47}$$

4) *ILs constraints*

Eq. (48) represents the maximum contingency reserve provided by IL. The maximum total schedulable load constraint of ILs is described by (49)

$$0 \leqslant R_{ILz,t}^{C} \leqslant IL_{z,\max}, \quad \forall\, t \in T, \forall\, z \in N_{IL} \tag{48}$$

$$\sum_{t=1}^{T} R_{ILz,t}^{C}\Delta t \leqslant Q_{ILz,\max}, \quad \forall\, z \in N_{IL} \tag{49}$$

5) *TUs constraints*

Eq. (50) enforces the upper and lower limits of power output of each TU. Eq. (51) enforces the ramping rate limits of each TU. Eq. (52)

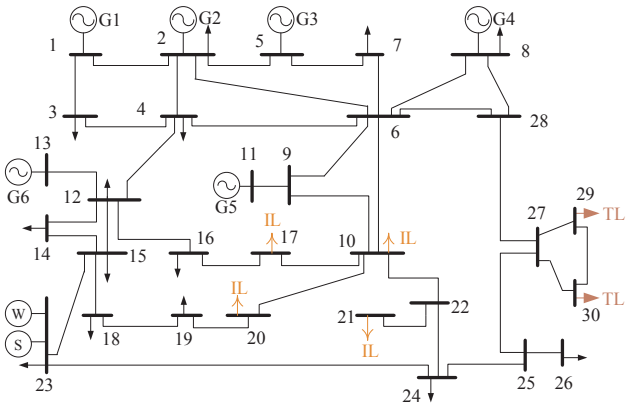

Fig. 3. One-line diagram of revised IEEE 30 bus system.

represents the minimum ON/OFF time restrictions. Eqs. (53) and (54) enforce the limits of the regulation and contingency reserves of each TU.

$$u_{Gi,t}P_{Gi,\min} \leqslant P_{Gi,t} \leqslant u_{Gi,t}P_{Gi,\max}, \quad \forall\, i \in N_G, \forall\, t \in T \tag{50}$$

$$\begin{cases} P_{Gi,t} - P_{Gi,t-1} \leqslant r_G^{up}\Delta t + (1-u_{Gi,t-1})P_{Gi,\max} \\ P_{Gi,t-1} - P_{Gi,t} \leqslant r_G^{down}\Delta t + (1-u_{Gi,t})P_{Gi,\max} \end{cases}, \quad \forall\, i \in N_G, \forall\, t \in T \tag{51}$$

$$\begin{cases} u_{Gi,t} - u_{Gi,t-1} - u_{Gi,r} \leqslant 0, & \forall\, r\colon 1 \leqslant r-(t-1) \leqslant \mathrm{M}_{Gi}^{ON}, \forall\, t \in T, \forall\, i \in N_G \\ u_{Gi,t-1} - u_{Gi,t} + u_{Gi,r} \leqslant 1, & \forall\, r\colon 1 \leqslant r-(t-1) \leqslant \mathrm{M}_{Gi}^{OFF}, \forall\, t \in T, \forall\, i \in N_G \end{cases} \tag{52}$$

$$\begin{cases} 0 \leqslant R_{Gi,t}^{Rup} \leqslant \min(P_{Gi,\max} - P_{Gi,t}, \Delta t_5 r_G^{up}) \\ 0 \leqslant R_{Gi,t}^{Rdown} \leqslant \min(P_{Gi,t} - P_{Gi,min}, \Delta t_5 r_G^{down}) \end{cases}, \quad \forall\, i \in N_G, \forall\, t \in T \tag{53}$$

$$0 \leqslant R_{Gi,t}^{C} \leqslant \min(P_{Gi,\max} - P_{Gi,t}, \Delta t_{15} r_G^{up}), \quad \forall\, i \in N_G, \forall\, t \in T \tag{54}$$

6) *Transmission line capacity constraint* [1]

$$-L_{l,\max} \leqslant F_{lb}P_t^b \leqslant L_{l,\max}, \quad \forall\, b \in B, \forall\, l \in L, \forall\, t \in T \tag{55}$$

4.4. Solving method

It can be observed from the AA-CAES operation constraints that, there are complex nonlinear relations between air pressure, temperature, power and mass flow rate. Therefore, the optimal scheduling problem with these constraints is a Mixed Integer Non-Linear Programming (MINLP) problem. However, the MINLP requires good knowledge of the problem and performance is affected by the starting points [39]. Compared to MINLP, Mixed Integer Linear Programming (MILP) problems are much easier to solve. The MILP algorithm may obtain good results with less computational time than nonlinear cases [39]. At present, the MILP has been widely used in the optimal scheduling of the power system with EES [31–33,39].

In order to linearize the model, the pressure ratio of the last compression stage is set to be the rated pressure ratio [31] and the temperature in the air reservoir is set to be the initial air temperature [11]. After that, the relationship between mass flow rate and air pressure change rate (Eq. (3)) is addressed using piecewise linear approximation.

Additionally, a set of binary variables is used to indicate the working mode conversion of AA-CAES when it provides reserve services. The stochastic chance constraints (41) and (42) are converted into their equivalent forms [40]:

$$\sum_{i=1}^{N_G} R_{Gi,t}^{Rup} + R_{CAES,t}^{Rup} \geqslant \Phi^{-1}(1-\mu)\sqrt{e_{L,t}^2 + e_{W,t}^2}, \quad \forall\, t \in T \tag{56}$$

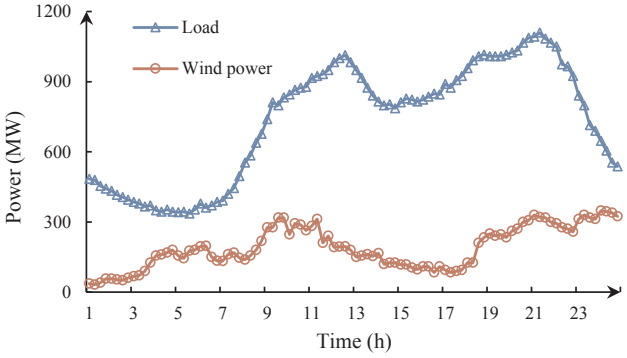

Fig. 4. Load and wind power forecast curves [42].

Table 1
Scheduling parameters of TUs [33].

Parameters	G1	G2	G3	G4	G5	G6
Max output (MW)	350	240	200	250	350	230
Min output (MW)	100	30	20	50	50	30
b_{Gi} ($/MW.h)	34.4	48.8	58.8	46.0	30.0	50.4
c_{Gi} ($/h)	130	110	120	110	120	100
Start-up cost ($)	1500	890	500	900	1450	720
Ramp up/down (MW/min)	2.3	4.5	8.2	4.6	2.7	7.9
Min ON/OFF time (h)	4	2	2	2	4	2
α_{Gi} ($/MW)	4.82	3.82	3.57	4.49	5.53	3.28
β_{Gi} ($/MW)	4.00	3.27	2.95	3.13	3.83	2.81
γ_{Gi} ($/MW)	3.80	4.02	3.55	3.82	3.42	3.65

$$\sum_{i=1}^{N_G} R_{Gi,t}^{Rdown} + R_{CAES,t}^{Rdown} \geqslant \Phi^{-1}(1-\mu)\sqrt{e_{L,t}^2 + e_{W,t}^2}, \quad \forall\, t \in T \tag{57}$$

After the above linearization and equivalent transformation processes, the optimal scheduling problem is converted into a MILP problem, which can be solve by conventional solvers efficiently. This paper uses the IBM ILOG CPLEX 12.6.3 to solve the MILP problem.

5. Case study

The case study illustrates the performance of the proposed scheduling model. The energy and reserve scheduling results of the power system with an AA-CAES are analysed. The impacts of AA-CAES on TUs and ILs schedules, energy and reserve costs, wind curtailment are analysed. The impacts of the maximum and minimum output of AA-CAES on reserve and energy costs are also studied.

5.1. Settings and assumptions

A revised IEEE 30 bus system is used for a case study. Fig. 3 illustrates the one-line diagram of the revised IEEE 30 bus system. An AA-CAES facility is located near a wind farm [22,23]. The wind farm and the AA-CAES facility are located at Bus 23 [33]. TLs and ILs are located in the load centre. Two TLs are located at Bus 29 and 30, and four ILs are located at Bus 10, 17, 20 and 21 [41].

In order to analyse and compare the impacts of AA-CAES, C-CAES and demand response programs on the power system scheduling, 4 scenarios are set. Scenario 1: There are no CAES facilities and demand response programs in the power system. Scenario 2: There is a C-CAES facility at bus 23; note that the gas consumption cost of C-CAES should be considered in the objective function in scenario 2. Scenario 3: There is an AA-CAES facility at bus 23. Scenario 4: There is an AA-CAES facility at bus 23. Also, two TLs are located at Bus 29 and 30, and four ILs are located at Bus 10, 17, 20 and 21.

The whole scheduling time is 24 h, and each time period is set to be 15 min. The forecasted load and wind power are shown in Fig. 4 [42].

Table 2
Scheduling parameters of AA-CAES [11,15,22].

Parameters	Value	Parameters	Value
Max/Min compressing power (MW)	100/60	Heat transfer coefficient α_h/β_h	0.24/0.015
Max/Min generating power (MW)	100/40	Cold/hot TES working medium temperature (K)	293/363
Number of the compressors/turbines	4	Max/Min pressure in air reservoir (bar)	55/40
Compression/Expansion pressure ratio	2.75/2.4	Initial temperature in air reservoir (K)	316
Efficiency to compressors/turbines	85%	Initial pressure in air reservoir (bar)	47.5
Max thermal storage capacity of TES (MJ)	2×10^6	Initial thermal storage capacity of TES	1×10^6
Average air temperature at the entrance of the air reservoir (K)	323	Ramp up/down rates in compressing/generating mode (MW/min)	40
Air reservoir volume (m^3)	4.8×10^5	b_{CAES} ($/MW.h)	28
$\alpha_{CAES}/\beta_{CAES}/\gamma_{CAES}$ ($/MW)	2.5/2/2.5	$\Delta t_{C,on}/\Delta t_{C,off}/\Delta t_{G,on}/\Delta t_{G,off}$ (min)	1.5

Table 3
Selected scheduling parameters of C-CAES [42].

Parameters	Value	Parameters	Value
The calorific value of gas (MJ/m^3)	38.8	Ramp up rates in generating mode (MW/min)	10
Combustion efficiency of gas (%)	85	$\alpha_{CAES}/\beta_{CAES}/\gamma_{CAES}$ ($/MW)	3/2.25/3
Unit price of gas ($/$m^3$)	0.2	$\Delta t_{G,on}$ (min)	2

The standard deviation of load and wind power forecast error are the 5% of forecast load and the 20% of forecast wind power output, respectively [41]. The Risk level is set to be 0.15. The scheduling parameters of TUs are shown in Table 1 [33].

The scheduling parameters of the AA-CAES facility are shown in Table 2 [11,15,22]. The scheduling parameters of C-CAES are shown in Table 3 [42]. The main difference between C-CAES and AA-CAES is that C-CAES has the gas combustion process while AA-CAES does not. Therefore, the generation start-up time of C-CAES is assumed to be longer and the cost coefficients of providing reserve services by C-CAES are assumed to be higher. The remaining scheduling parameters of C-CAES are assumed to be the same as the parameters of AA-CAES [16].

The scheduling parameters of the two TLs are assumed to be the same. The TLs are schedulable at 0:00–12:00. The maximum load increment and reduction of the TLs are both 20 MW. The maximum total schedulable load of a TL is 40 MW.h. The load-shifting cost of a TL is set to be 4.8 $/(MW.h). The scheduling parameters of the four ILs are also assumed to be the same. The maximum contingency reserve of an IL is 15 MW. The maximum total schedulable load of an IL is set to be 90 MW.h. The cost of providing contingency reserve of an IL is set to be 3.6 $/(MW) [41].

5.2. Results and analysis

1) Scheduling results of the power system with AA-CAES (scenario 4)

The generation schedules are shown in Fig. 5(a). The upward and downward regulation reserve schedules are shown in Fig. 5(b) and (c), respectively. The contingency reserve schedules are shown in Fig. 5(d). The AA-CAES compressing power is represented by negative generating power.

G1 and G5, which can provide cheaper energy, are dispatched to supply the most of the electricity demand. G3 and G6 have higher ramp up/down rates and relatively cheaper reserve costs; G3 is mainly dispatched to provide contingency reserve service and G6 plays a major role in providing both regulation and contingency reserves services. G2 and G4 are never committed because they do not have obvious advantages in generation or providing reserve services. TLs are scheduled to provide load shifting service, while ILs are scheduled to undertake a small part of the system contingency reserve demand. The AA-CAES facility has the best dynamic characteristics and the cheapest reserve costs; it undertakes a large proportion of system reserve demand and

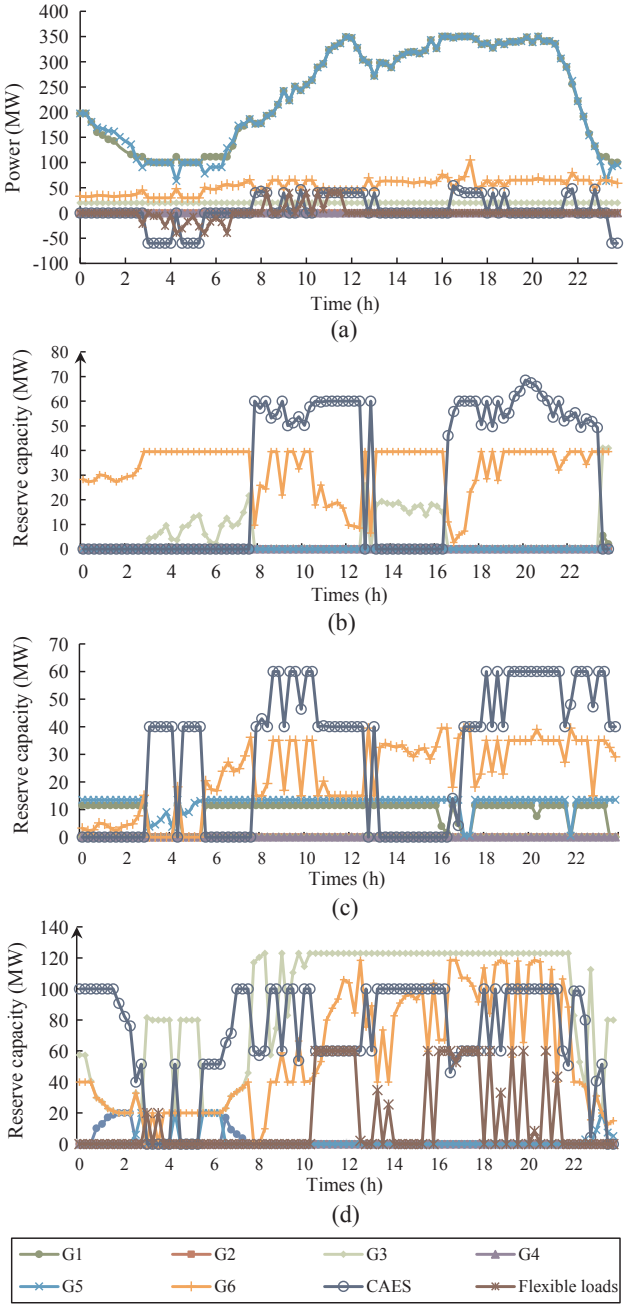

Fig. 5. (a) Generation schedules; (b) Upward regulation reserve schedules; (c) Downward regulation reserve schedules; (d) Contingency reserve schedules.

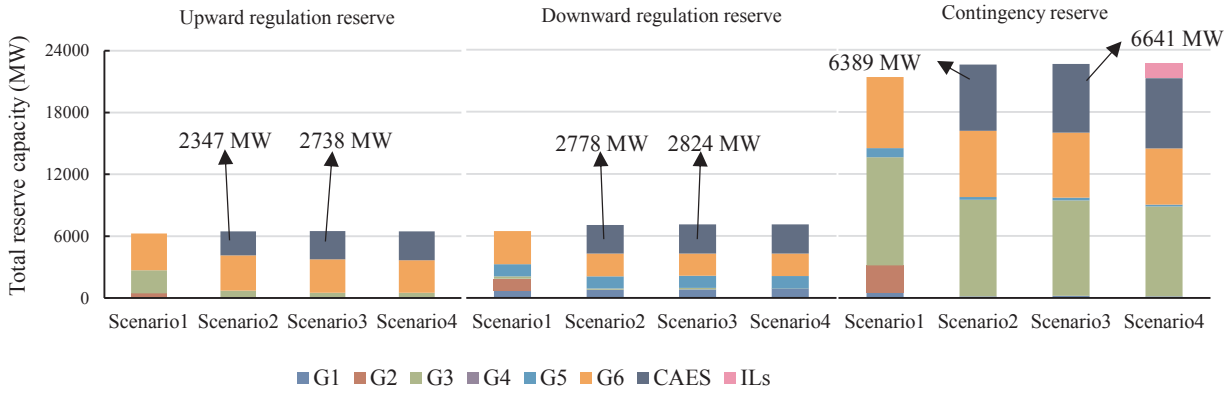

Fig. 6. Total reserves provided by each scheduling resource in four scenarios.

Table 4
Costs in four scenarios.

Costs	Scenario 1	Scenario 2	Scenario 3	Scenario 4
Energy cost of TUs ($)	512,119	472,422	472,302	470,032
Energy cost of CAES ($)	—	11,488	7706	7581
Regulation reserve cost of TUs ($)	43,006	27,940	26,768	26,580
Regulation reserve cost of CAES ($)	—	12,900	12,493	12,660
Contingency reserve cost of TUs ($)	77,734	58,053	57,415	51,933
Contingency reserve cost of CAES ($)	—	19,168	16,602	16,929
Cost of scheduling TLs and ILs ($)	—	—	—	5558
Penalty of wind curtailment ($)	69,584	0	0	0
System total cost ($)	702,443	601,971	593,286	591,273

has the ability of shifting load from peak to valley.

However, a shortcoming of AA-CAES is that the regulation range of AA-CAES reserve capacity is not continuous. This makes the AA-CAES facility unsuitable for undertaking system reserve demand alone and forces the TUs and ILs to provide enough reserve to fill in the "blanks". As can be seen in Fig. 5(b)–(d), AA-CAES almost never undertakes system reserve demand alone. Furthermore, during the periods of low system reserve demand, the extra costs, which are caused by TUs providing extra regulation reserves to fill in the "blanks", may be greater than the benefits of using the regulation reserve services of AA-CAES. Therefore, it may not be a good choice for AA-CAES to provide reserve services during the periods of low system reserve demand (see hours 1–3 and 15–18 in Fig. 5(b) and (c)).

According to Fig. 5(a), the times that the AA-CAES facility is under idling mode is nearly 60% of a day. Even when the AA-CAES facility is under compression or generation modes, its compressing or generating power is close to the lower limits. That is mainly because: 1) In the power system described in section 4.1, the AA-CAES facility has an obvious advantage in providing reserve services. 2) When the AA-CAES facility is under idling mode or operating at the minimum compressing/generating power, it has great potential in providing both upward reserves (upward regulation reserve and contingency reserve) and downward reserve (downward regulation reserve).

2) Impacts of AA-CAES, C-CAES and demand response programs on power system schedules

The total reserves provided by each scheduling resource in a day are

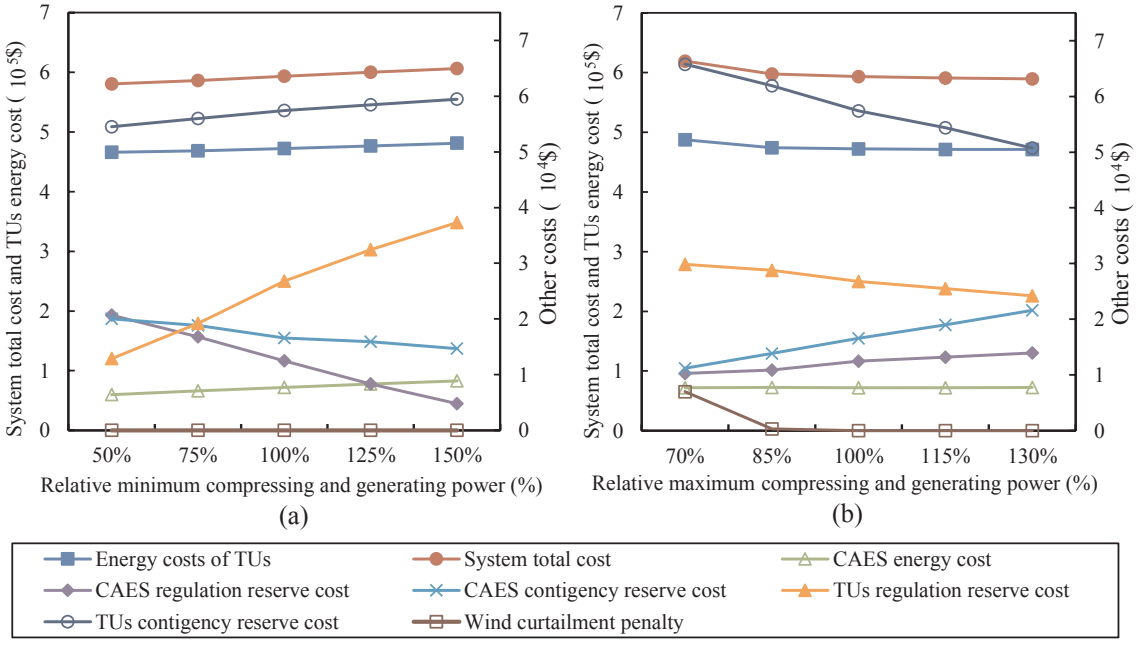

Fig. 7. (a) Trend of costs with different minimum AA-CAES output limits; (b) Trend of costs with different maximum AA-CAES output limits.

shown in Fig. 6. In Fig. 6, the total upward regulation reserves of AA-CAES and TU i in a day are calculated by $\sum_{t=1}^{T} R_{CAES,t}^{Rup}$ and $\sum_{t=1}^{T} R_{Gi,t}^{Rup}$ respectively; the total downward regulation reserves of AA-CAES and TU i in a day are calculated by $\sum_{t=1}^{T} R_{CAES,t}^{Rdown}$ and $\sum_{t=1}^{T} R_{Gi,t}^{Rdown}$ respectively; the total contingency reserves of AA-CAES, TU i and ILs in a day are calculated by $\sum_{t=1}^{T} R_{CAES,t}^{C}$, $\sum_{t=1}^{T} R_{Gi,t}^{C}$ and $\sum_{z=1}^{N_{IL}} \sum_{t=1}^{T} R_{ILz,t}^{C}$ respectively.

From Fig. 6, the total upward regulation reserve, downward regulation reserve and contingency reserve provided by AA-CAES in scenario 3 are increased by 16.7%, 1.7% and 3.9% of the corresponding reserves provided by C-CAES in scenario 2, respectively. It indicates that, compared to C-CAES, the advantages of AA-CAES in providing upward regulation reserve service are more obvious than providing other kinds of reserve services. That is mainly because: 1) there is no fuel combustion process in the generation mode of AA-CAES. Therefore, AA-CAES is more flexible than C-CAES in upward power regulation. Moreover, it costs less in providing upward reserve service. 2) The response time of providing regulation reserve service (5 min) is shorter than the response time of providing contingency reserve service (15 min). Therefore, the advantages of AA-CAES such as high ramp-up rate and fast generation start-up are more significant in providing upward reserve service.

It can also be observed from Fig. 6 that the total upward regulation reserve, downward regulation reserve and contingency reserve provided by CAES, TUs and ILs in scenarios 2, 3 and 4 are all greater than the corresponding reserves in scenario 1. That is because the regulation range of the reserves provided by the CAES is not continuous, so that the TUs and ILs have to provide more reserves. However, according to Table 4, which shows the costs in four scenarios, the total reserve cost (sum of regulation reserve costs and contingency reserve costs) in scenarios 2, 3 and 4 is much less than the total reserve cost in scenario 1. This is due to the good dynamic characteristics of CAES and the relatively lower cost in providing reserves with CAES.

Comparing the results in scenario 3 and 4, the demand response programs hardly effect the total contingency reserve of AA-CAES, but the total contingency reserve provided by TUs is decreased.

It can be seen from Table 4 that, compared with the system total cost in scenario 1, the system total costs in scenarios 2 and 3 decrease about 14.3% and 15.5% respectively, and there is no wind curtailment in scenarios 2 and 3. The results indicate that both AA-CAES and C-CAES can increase the system operation economy and mitigate wind curtailment, but AA-CAES preforms better in reducing system total cost than C-CAES. Additionally, the system total cost in scenario 4 is the lowest.

Moreover, the total energy cost (sum of the energy costs of CAES and TUs) and the energy cost of TUs in scenario 3 decrease about 6.3% and 7.8% compared with the corresponding costs in scenario 1. The reason is that: the proportion of system reserve demand undertaken by TUs is decreased after the AA-CAES facility participates in reserve markets, so that the number of the TUs, which are in the ON state, can be reduced. Therefore, the TUs with bad operation economy can be shut down and the energy cost of TUs is reduced.

3) Impacts of the AA-CAES's maximum and minimum output limits on costs (based on scenario 3)

Fig. 7(a) shows the trend of the costs when the minimum compressing and generating powers are changed by the same proportion simultaneously. Fig. 7(b) shows the trend of the costs when the maximum compressing and generating powers are changed by the same proportion simultaneously (other parameters of AA-CAES remain unchanged).

Fig. 7(a) and (b) indicate that the system total cost can be reduced by reducing the minimum output power and increasing the maximum output power of AA-CAES. Besides, Fig. 7(b) indicates that the reduction of the maximum output limits of AA-CAES may cause wind curtailment.

From Fig. 7(a), with the increasing of the minimum output limits, the regulation and contingency reserve costs of AA-CAES are decreasingly obviously, while the regulation and contingency reserve costs of TUs have an increasing trend. The reason is that: with the increasing of the minimum output limits, the unfeasible regulation range of the reserves provided by AA-CAES is enlarging. Therefore, the AA-CAE facility is dispatched to undertake less reserve demand.

Fig. 7(b) shows the opposite result: with the increasing of the maximum output limits, the reserve costs of AA-CAES is getting higher.

6. Conclusion

This paper presents a reserve capacity model of AA-CAES for power system optimal joint energy and reserve scheduling. The model takes the practical limitations and operation characteristics of AA-CAES into account. Additionally, the limitations on TUs and ILs reserve capacities caused by AA-CAES are considered in the power system optimal scheduling. Based on the numerical simulations results, several conclusions can be drawn: (1) The participation of AA-CAES in power system scheduling can reduce the system energy and reserve costs and can mitigate wind curtailment. (2) AA-CAES is not suitable for undertaking the system reserve demand alone. Using AA-CAES to provide reserve services may increase the total reserve demand of the power system, but the total system reserve cost can still be reduced due to the good dynamic characteristics and low reserve costs of AA-CAES. (3) Compared to C-CAES, the advantage of AA-CAES in providing upward regulation reserve service is more obvious than in providing downward regulation reserve service and contingency reserve service. AA-CAES also performs better in reducing the system total cost than C-CAES. (4) With the increasing of AA-CAES minimum output, the advantage of AA-CAES in providing reserve services is weakening. On the contrary, the increasing of AA-CAES maximum output enhances the advantage of AA-CAES in providing reserve services.

Note that the scheduling models of CAES proposed in this paper are used for power system day-ahead scheduling. They are not suitable for the power system real-time dispatch because the time scales and main focuses of the day-ahead scheduling and real-time dispatch are different. It is planned future work to study the real-time dispatch model of CAES. In addition, since the construction and investment costs do not need to be considered in the day ahead scheduling, the proposed models are not suitable for the economic analysis of CAES. In the future, the economic analysis of different large scale EES technologies can also be carried out.

Acknowledgment

The authors would like to thank the research grant support from The National Key Research and Development Program of China (2017YFB0903601) and The National Natural Science Foundation of China (51777088).

References

[1] Zhao C, Wang J, Watson JP, et al. Multi-Stage Robust Unit Commitment Considering Wind and Demand Response Uncertainties. IEEE Trans Power Syst 2013;28(3):2708–17.
[2] Park H, Baldick R. Integration of compressed air energy storage systems co-located with wind resources in the ERCOT transmission system. Int J Electr Power Energy Syst 2017;90:181–9.
[3] Beaudin M, Zareipour H, Schellenberglabe A, et al. Energy storage for mitigating the variability of renewable electricity sources: An updated review. Energy Sustain Dev 2010;14(4):302–14.
[4] Chazarra M, Perez-Diaz J I, Garcia-Gonzalez J. Optimal Joint Energy and Secondary Regulation Reserve Hourly Scheduling of Variable Speed Pumped Storage Hydropower Plants. IEEE Trans Power Syst 2017, PP(99):1–1.
[5] Aissou S, Rekioua D, Mezzai N, et al. Modeling and control of hybrid photovoltaic wind power system with battery storage. Energy Convers Manage 2015;89(89):615–25.

[6] Benato A, Stoppato A. Energy and cost analysis of an Air Cycle used as prime mover of a Thermal Electricity Storage. J Storage Mater 2018;17:29–46.
[7] Frate GF, Antonelli M, Desideri U. A novel Pumped Thermal Electricity Storage (PTES) system with thermal integration. Appl Therm Eng 2017;121.
[8] Benato A. Performance and cost evaluation of an innovative Pumped Thermal Electricity Storage power system. Energy 2017;138.
[9] Sciacovelli A, Vecchi A, Ding Y. Liquid air energy storage (LAES) with packed bed cold thermal storage – From component to system level performance through dynamic modelling. Appl Energy 2017;190:84–98.
[10] He W, Wang J, Ding Y. New radial turbine dynamic modelling in a low-temperature adiabatic Compressed Air Energy Storage system discharging process. Energy Convers Manag 2017;153:144–56.
[11] Raju M, Khaitan SK. Modeling and simulation of compressed air storage in caverns: a case study of the Huntorf plant. Appl Energy 2012;89(1):474–81.
[12] China Industrial Association., Research report of energy storage application industry in China, (China Industrial Association of Power Sources, 2016), pp. 21–48.
[13] Chen L, Zheng T, Mei S, et al. Review and prospect of compressed air energy storage system. J Mod Power Syst Clean Energy 2016;4(4):529–41.
[14] Cleary B, Duffy A, Oconnor A, et al. Assessing the Economic Benefits of Compressed Air Energy Storage for Mitigating Wind Curtailment. IEEE Trans Sustain Energy 2015;6(3):1021–8.
[15] Luo X, Wang J, Krupke C, et al. Modelling study, efficiency analysis and optimisation of large-scale Adiabatic Compressed Air Energy Storage systems with low-temperature thermal storage. Appl Energy 2016;162:589–600.
[16] Mei S, Wang J, Tian F, et al. Design and engineering implementation of non-supplementary fired compressed air energy storage system: TICC-500. Sci China 2015;58(04):600–11.
[17] Overview of research institute 12th five-year key cultivation direction progress, http://www.iet.cas.cn/hdzt/135zl/2016yisanwu/201605/t20160524_4608819.html, accessed 27 November 2014.
[18] Wang J, Lu K, Ma L, et al. Overview of Compressed Air Energy Storage and Technology Development. Energies 2017;991(10):1–22.
[19] Nojavan S, Najafi-Ghalelou A, Majidi M, Zare K. Optimal bidding and offering strategies of merchant compressed air energy storage in deregulated electricity market using robust optimization approach. Energy 2018 Jan;1(142):250–7.
[20] Shafiee S, Zareipour H, Knight AM, Amjady N, Mohammadi-Ivatloo B. Risk-constrained bidding and offering strategy for a merchant compressed air energy storage plant. IEEE Trans Power Syst 2017 Mar;32(2):946–57.
[21] Shafiee S, Zareipour H, Knight AM. Developing Bidding and Offering Curves of a Price-maker Energy Storage Facility Based on Robust Optimization. IEEE Trans Smart Grid, 2017, PP(99):1–1.
[22] Li Y, Miao S, Luo X, et al. Optimization model for the power system scheduling with wind generation and compressed air energy storage combination'. IEEE Int Conf Autom Comput, Colchester, UK September 2016, 300–305.
[23] Attarha A, Amjady N, Dehghan S, et al. Adaptive Robust Self-scheduling for a Wind Producer with Compressed Air Energy Storage. IEEE Trans Sustain Energy 2018, PP(99):1–1.
[24] Wang C, Chen L, Liu F, et al. Thermal-wind-storage joint operation of power system considering pumped storage and distributed compressed air energy storage. Power Systems Computation Conference. IEEE, 2015:1–7.
[25] Abbaspour M, Satkin M, Mohammadi-Ivatloo B, et al. Optimal operation scheduling of wind power integrated with compressed air energy storage (CAES). Renew Energy 2013;51(51):53–9.
[26] Ghalelou A, Fakhri A, Nojavan S, et al. A stochastic self-scheduling program for compressed air energy storage (CAES) of renewable energy sources (RESs) based on a demand response mechanism. Energy Convers Manag 2016;120:388–96.
[27] Daneshi H, Srivastava AK. Security-constrained unit commitment with wind generation and compressed air energy storage. IET Gener Transm Dis 2013;6(2):167–75.
[28] Ghaljehei M, Ahmadian A, Golkar MA, et al. Stochastic SCUC considering compressed air energy storage and wind power generation: a techno-economic approach with static voltage stability analysis. Int J Electr Power Energy Syst 2018.
[29] Drury E, Denholm P, Sioshansi R. The value of compressed air energy storage in energy and reserve markets. Energy 2011;36(8):4959–73.
[30] Ruiz PA, Sauer PW. Spinning Contingency Reserve: Economic Value and Demand Functions. IEEE Trans Power Syst 2008;23(3):1071–8.
[31] Rui L, Chen L, Yuan T, et al. Optimal dispatch of zero-carbon-emission micro Energy Internet integrated with non-supplementary fired compressed air energy storage system. J Mod Power Syst Clean Energy 2016;4(4):566–80.
[32] Shafiee S, Zareipour H, Knight A. Considering thermodynamic characteristics of a CAES facility in self-scheduling in energy and reserve markets. IEEE Trans Smart Grid, 2016, early acess.
[33] Luo C, Yang J, Sun Y, et al. Dynamic economic dispatch of wind integrated power system considering optimal scheduling of reserve capacity. Proc CESS 2014;34(34):6109–18.
[34] Wu W, Zhang B, Chen J, et al. Multiple time-scale coordinated power control system to accommodate significant wind power penetration and its real application. Power and Energy Society General Meeting. IEEE, 2012:1–6.
[35] Zhang X. Multistage radial turbine for supercritical compressed air energy storage system. University of chinese academy of sciences, 2014.
[36] Mohsenian-Rad H. Optimal Demand Bidding for Time-Shiftable Loads. IEEE Trans Power Syst 2015;30(2):939–51.
[37] Sousa J, Saavedra O R, Lima S L. Decision-Making in Emergency Operation for Power Transformers with Regard to Risks and Interruptible Load Contracts. IEEE Trans Power Deliv 2017, PP(99):1–1.
[38] Wu H, Shahidehpour M, Li Z, et al. Chance-Constrained Day-Ahead Scheduling in Stochastic Power System Operation. IEEE Trans Power Syst 2014;29(4):1583–91.
[39] Chen CH, Chen N, Luh PB. Head Dependence of Pump-Storage-Unit Model Applied to Generation Scheduling. IEEE Trans Power Syst 2017;32(4):2869–77.
[40] Wu H, Shahidehpour M, Li Z, et al. Chance-constrained day-ahead scheduling in stochastic power system operation. IEEE Trans Power Syst 2014;29(4):1583–91.
[41] Bao Y, Wang B, Li Y, et al. Rolling dispatch model considering wind penetration and multi-scale demand response resources. Proc CESS 2016;36(17):4589–99.
[42] Li Y, Miao S, Luo X, et al. Day-ahead and Intra-day Time Scales Coordinative Dispatch Strategy of Power System with Compressed Air Energy Storage. Proc. CESS, 2018, early acess.